PNL-9415
UC-603

Subcontractor Report

Regional Forecasting With Global Atmospheric Models

Fourth Year Report

May 1994

Prepared by Applied Research Corporation
for Pacific Northwest Laboratory
under Contract DE-AC06-76RLO 1830
with the U.S. Department of Energy

Pacific Northwest Laboratory
Operated for the U.S. Department of Energy
by Battelle Memorial Institute

Battelle

PNL-9415

DISCLAIMER

PACIFIC NORTHWEST LABORATORY
operated by
BATTELLE MEMORIAL INSTITUTE
for the
UNITED STATES DEPARTMENT OF ENERGY
under Contract DE-AC06-76RLO 1830

Printed in the United States of America

Available to DOE and DOE contractors from the Office of Scientific and Technical Information, P.O. Box 62, Oak Ridge, TN 37831; prices available from (615) 576-8401. FTS 626-8401.

Available to the public from the National Technical Information Service, U.S. Department of Commerce, 5285 Port Royal Rd., Springfield, VA 22161.

PNL-9415
UC-603

REGIONAL FORECASTING WITH GLOBAL ATMOSPHERIC MODELS

FOURTH YEAR REPORT

Thomas J. Crowley
Gerald R. North
Neil R. Smith

Applied Research Corporation
College Station, Texas

W. H. Walters, PNL Project Manager

May 1994

Prepared by Applied Research Corporation
for Pacific Northwest Laboratory
under Contract DE-AC06-76RLO 1830
with the U.S. Department of Energy

Pacific Northwest Laboratory
Richland, Washington 99352

FOREWORD

This report was prepared by the Applied Research Corporation (ARC), College Station, Texas, under subcontract to Pacific Northwest Laboratory (PNL) as part of a global climate studies task. The task supports site characterization work required for a high-level nuclear waste repository and is part of the Performance Assessment Scientific Support (PASS) Program at PNL, which is under the direction of the Yucca Mountain Project Office (YMPO), Las Vegas, Nevada. The work is under the overall direction of the Office of Civilian Radioactive Waste Management (OCRWM), U.S. Department of Energy Headquarters, Washington, D.C.

The scope of the report is to present the results of the fourth year's work on the atmospheric modeling part of the global climate studies task. The development testing of computer models and initial results are discussed. The appendices contain studies that provide supporting information and guidance to the modeling work and further details on computer model development. Complete documentation of the models, including user information, will be prepared under separate reports and manuals.

The task work involves the services of two other subcontractors: The University of Maine (UM), Orono, Maine (global ice sheet modeling), and the Lamont-Doherty Geological Observatory (LDGO), Palisades, New York (global climate data base development). The studies by UM and LDGO directly support the atmospheric modeling effort and are reported separately by the respective contractor.

SUMMARY

The Applied Research Corporation (ARC) conducted this study for the Pacific Northwest Laboratory (PNL). The purpose of the study is to make regional forecasts of climate change in order to ensure the long-term security of nuclear waste disposal sites.

In this report we review progress toward implementing a plan for making future forecasts. The plan is based on the recognition of a need to develop a hierarchical climate modeling approach, utilizing both simple and complex models. The plan also recognizes that before we can predict future climates with confidence, we must demonstrate some skill in predicting past climates.

At the end of Year Four, the following accomplishments can be noted as follows:

- modified work plan for Year Four as a result of a 60% cutback in budget
- compared the sensitivity of an energy balance model to historical temperature fluctuations to determine whether the model and observations have the same sensitivity
- developed a new energy balance model in order to examine time varying changes in temperature during the next 100 years
- staff underwent training for the use of new general circulation model developed at National Center for Atmospheric Research (NCAR) to be used by ARC
- acquired some information on non-PNL funded activities that will help strengthen and sharpen the climate plan for Yucca Mountain
- completed Quality Assurance (QA) documentation of fourteen software codes, enhanced data base structures, and prepared for acquisition and modification of the University of Maine ice boundary conditions.

CONTENTS

FIGURES

TABLES

1.0 INTRODUCTION

Applied Research Corporation (ARC) is pleased to submit its fourth year report on "Regional Forecasting With Global Atmospheric Models", Pacific Northwest Laboratory (PNL) Contract No. 017113-A-B1. We have been involved in a number of activities, and this overview will summarize our work and include selected references to earlier work accomplished during the first three years of the project. Detailed technical discussions are included as separate appendices.

Our work has covered six main topics: (1) modification of work plan to accommodate budget reductions; (2) comparison of energy balance model (EBM) simulation with observations in order to determine whether models and observations have the same sensitivity; (3) developed a new energy balance model in order to examine the time-dependent problem of global warming; (4) subjected staff to training session at NCAR for purposes of using their general circulation model (GCM); (5) acquired new information relevant to strengthening and sharpening the Site Characterization Plan for Climate Studies; (6) Completed a backlog of QA activities, essentially bringing this element of our program up-to-date with existing research activities. Our summary will discuss these activities in the same order.

2.0 MODIFICATION OF WORK PLAN

Although our original work plan called for ARC to initiate general circulation modeling (GCM) activities in Year Four of the project, an unexpected budget cutback (60%) greatly affected this goal and required modification of the work plan for Year Four. As a result of the cutback, two employees were released, one was cut back and shifted primarily to another project, and a fourth was shifted to another project for part of the time.

Because of these reductions there were two major modifications to the Year Four work plan: (1) we greatly reduced, to the point of abandonment, work on the low-resolution GCM because of loss of an employee and because the additional year's delay in activities would have otherwise caused the same delay in completion of the overall project; (2) we restricted our activities mainly to: (a) energy balance model (EBM) comparisons with observations, with the purpose being determining whether the EBM has the same sensitivity as observations; (b) development of a new EBM that allows us to look at the time-varying changes in temperature over the next 100 years due to greenhouse warming; (c) catching up on Quality Assurance (QA) utilities. Points (a), (b), and (c) will be further developed in Sections 3.0, 4.0, and 7.0.

3.0 EBM MODEL-DATA COMPARISONS

One of the stated purposes of our hierarchical approach to climate modeling is that EBMs can be used to scope out the range of possible topics for GCM activities. Although the EBM agrees well with the GCM for "hindcast" climate simulations of the last 18,000 years (e.g. Figure 1), this agreement does not necessarily mean that either model would agree with observations. Accordingly, K.-Y. Kim and G. North undertook modifications of our EBM to generate results that could be compared directly with observations of temperature fluctuation over part of the present century. This exercise is a more rigorous test of our conjecture about possibly substituting EBM SST fields as input in GCM runs.

The basic model modification involved "stochastic" or noise forcing of our previously developed EBM (Hyde et al. 1989). When the model-generated output is compared with observations, which include weather variations we cannot explicitly include in the EBM, then we are able to test whether the model has the same sensitivity as the observations.

Results (Figures 2 and 3) are very promising. In the first case (Figure 2) we compared the spectrum of the model response to the observed temperature fluctuations of the last 40 years. In the second case (Figures 3 and 4) we made a spatial comparison of the model's and observation's responses. In this latter case, there are many areas where the model and observations have similar statistics. A major difference involves changes in equatorial Pacific SSTs (El Nino), which the model cannot be expected to capture (Figure 4). Overall, however, the comparison is very favorable and further justifies our use of EBMs on the project.

A write-up of the results has been submitted to the *Journal of Geophysical Research* and is reproduced in Appendix A.

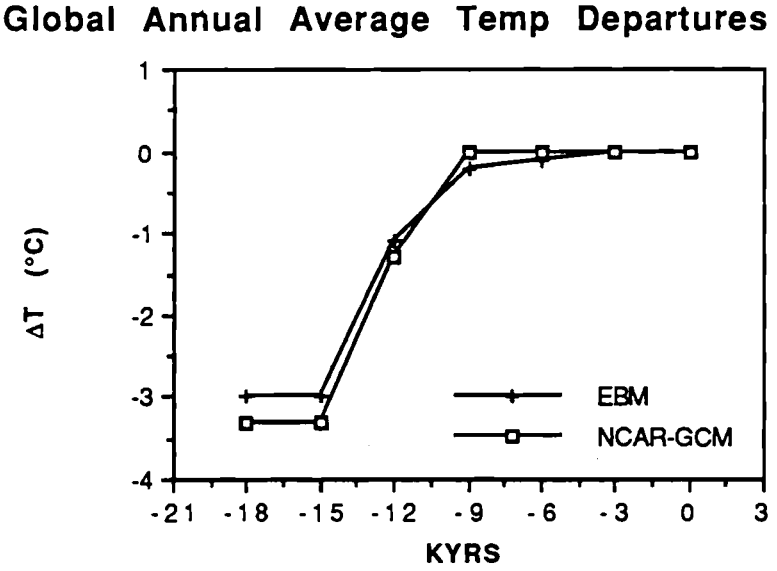

a) Present CO_2 levels

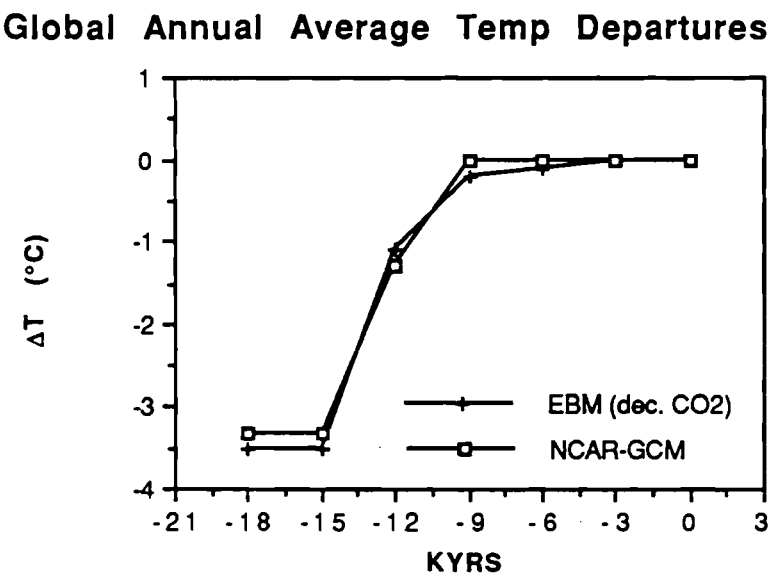

b) 15,18 ka CO_2 levels

FIGURE 1. Comparison of EBM and GCM Estimates of Global Annual Average Temperature Departures over the Ocean for the Past 18,000 Years. Comparison using a) the present value of CO_2 concentration in a linear energy balance model; and b) with decreased CO_2 concentrations at 15 and 18 kyrs before present (ka). Over the open ocean, the NCAR-GCM values are the estimates by CLIMAP Project Members (1981). [From Hyde et al. 1989]

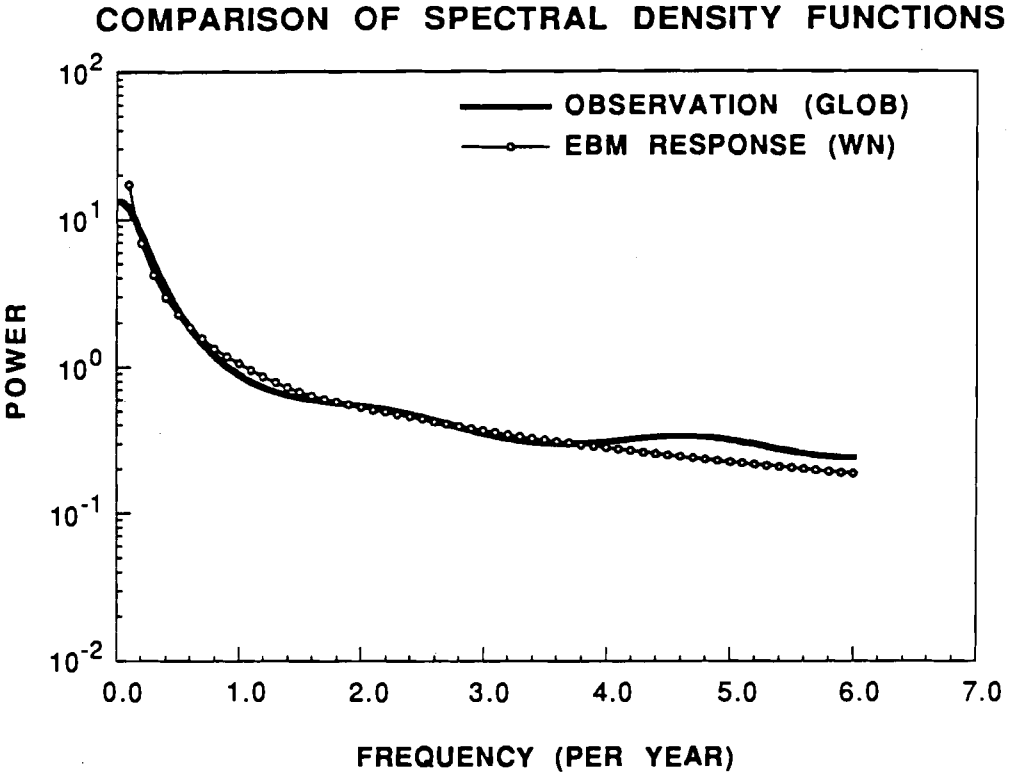

FIGURE 2. Spectral Density Functions of the Global Average Temperatures: thick line - observation (auto-regressive fitting of order 5); thin line with circle - linear energy balance model response to a noise forcing white in space and time. [From Appendix A]

One of the problems that still has to be addressed in GCM studies involves the need to use a mixed-layer ocean model for making the proposed eight runs with the NCAR GCM (see appendix B for definition of model terms). Such an approach would require approximately 180 hours of Cray time per run. The costs could rapidly exceed our ability to pay for them. We have therefore been exploring the possibility of utilizing the EBM to generate sea-surface temperatures (SSTs), which can then be used as input to the GCM so that it can be run with fixed (or prescribed) SSTs. Such an approach would greatly shorten the run times.

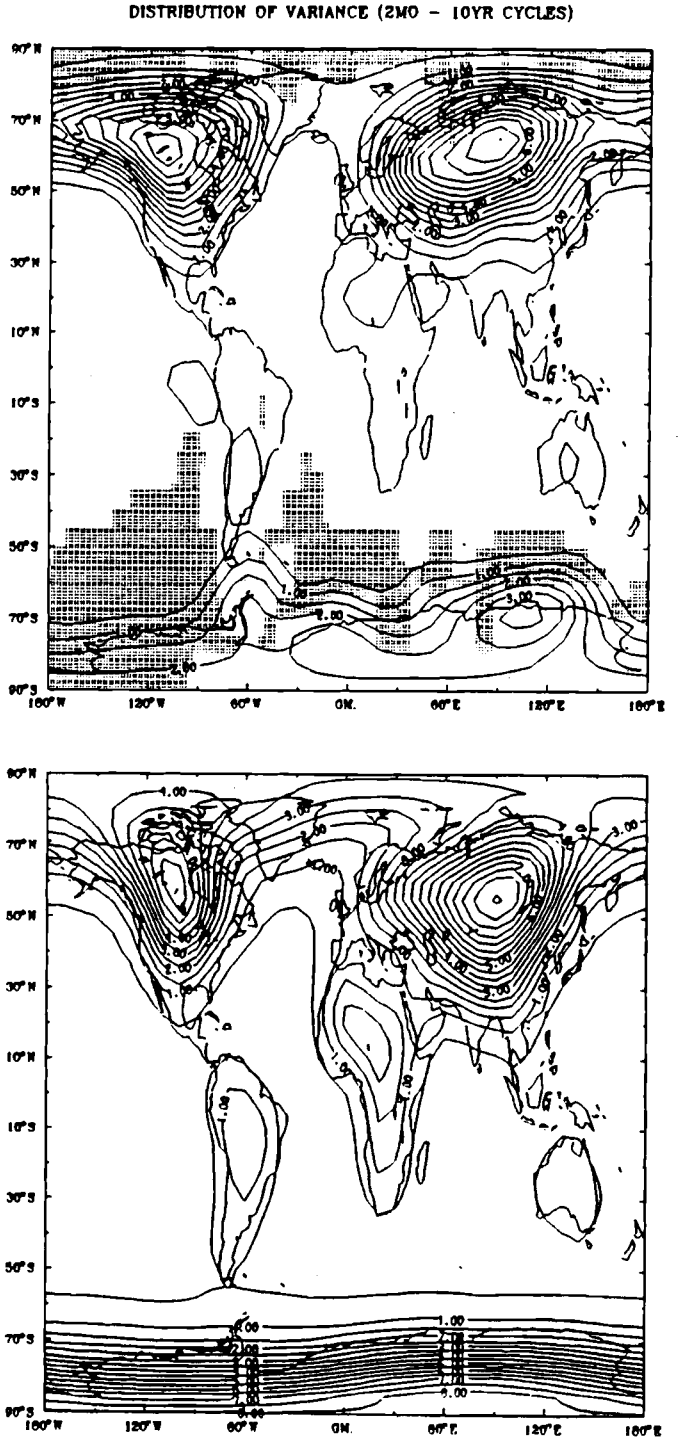

FIGURE 3. Geography of the Distribution of Variance ($°C^2$) Within Frequency Band of Period 2 month - 10 year: a) Observations (shaded areas indicate regions with less than 30 years of data available); b) Linear Energy Balance Model with a Noise Forcing white in space and time. [From Appendix A]

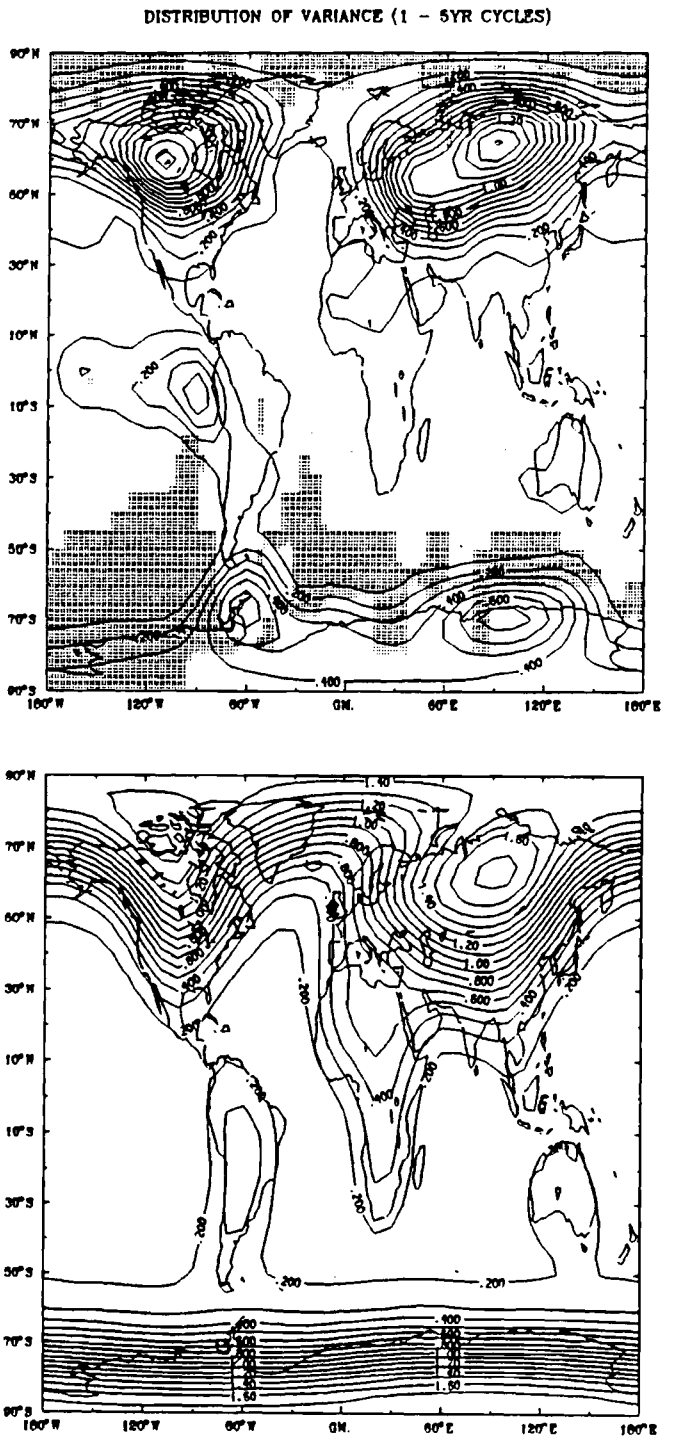

FIGURE 4. Geography of the Distribution of Variance Within 1 - 5 year Band: a) Observations (shaded areas indicate regions with less than 30 years of data available); b) Linear Energy Balance Model with a Noise Forcing white in space and time. [From Appendix A]

Since our earlier work indicated a surprising level of fidelity between EBMs and GCMs (Figure 1) we have been encouraged to consider using EBMs to help constrain some of the boundary conditions for our future GCM runs. In particular, we are interested in sea-surface temperatures (SSTs), as it is well known that calculation of SSTs in a GCM increases computation time (and costs) by an order of magnitude. If we can use an EBM to generate SSTs and then run the GCM with these "prescribed" SSTs, then we can save greatly on computer costs.

For our approach to be valid, we not only have to validate our EBM against GCMs to test our SST field (Figure 1), we also have to test them against observations. Our initial testing of this hypothesis is illustrated in Figure 5, which compares the EBM model generated SST field (from Hyde et al. 1990; see also Crowley et al. 1990, Appendix D) with observations of latitudinally-averaged SST. Overall, the comparison is quite favorable except in August, when the EBM underestimates SSTs in the Northern Hemisphere. We conjecture that this effect is due to lack of a Gulf Stream in the model. One way we may address this problem is to prescribe a heat source in the model to mimic a Gulf Stream effect. This approach is also taken by GCM groups, who sometimes cannot explicitly incorporate the effects of the ocean circulation. Although further testing on this subject is warranted, results are sufficiently promising to encourage us to consider use of EBMs to stipulate SSTs for future GCM runs.

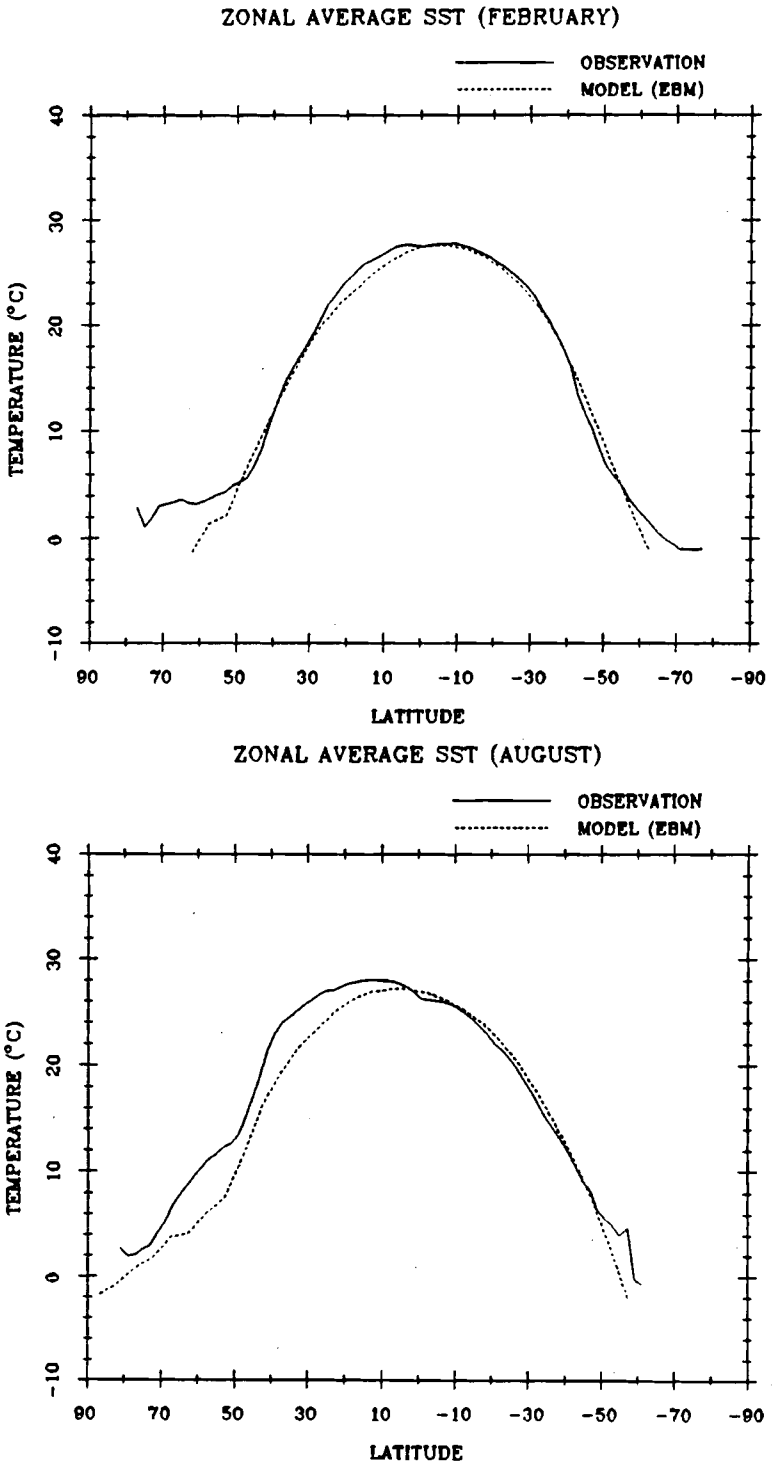

FIGURE 5. Comparison of Model-Generated Zonally-Averaged SSTs with Observations. These results suggest that EBMs can be used to stipulate the SST field in future GCM runs.

4.0 DEVELOPMENT OF NEW ENERGY BALANCE MODEL

Because we were unable to initiate GCM studies in Year Four, ARC undertook development of a new EBM that would investigate the time varying changes in forcing over the next 100 years. This problem, termed "transient CO_2 forcing" in the literature, is of interest because it examines the nonequilibrium climate response to CO_2 changes (most other simulations involved equilibrium runs -- see Schlesinger 1988 for a review). It is of direct interest to Yucca Mountain because it encompasses the time interval over which the site will be monitored and nuclear waste can be retrieved.

Although work has started on coupled ocean-atmosphere GCM experiments for the transient CO_2 problem (e.g., Washington and Meehl 1989; Manabe et al. 1990; Cubasch et al. 1991), it is still of interest to explore the phenomenon in an EBM for some of the same reasons we conducted other EBM-GCM comparisons. In order to address the problem of the transient CO_2 warming, it is necessary to include the effects of the deep-ocean circulation, because slow upwelling of deep waters regulates the time evolution of temperature. Accordingly, ARC has utilized some of the simple global-averaged model methods of Hoffert and Flannery (1985) and Morantine and Watts (1990), coupling their deep-ocean term to the two-dimensional EBM previously developed under the PNL contract (Hyde et al. 1989).

At present we are still in the testing stage for the model and have no reportable results. However, in the future we hope to conduct some comparisons with the Hamburg coupled ocean-atmosphere model simulation (Cubasch et al. 1991). The later model, developed at the Max Planck Institute (MPI), may also prove useful in more sharply framing our attack on one of the more difficult problems of our forecast experiments (see Section 6.0).

5.0 EMPLOYEE TRAINING ON THE NEW NCAR GCM

Although we were not able to conduct any GCM simulations, ARC took the step of preparing for that eventuality in Year Five of our project by ensuring that relevant employees received training on the new version of the NCAR GCM developed by S. Thompson (and to be used by them on the Yucca Mtn. project under separate funding by Sandia National Laboratory). We have taken two steps in that direction. Via remote access to NCAR we have been training an employee on testing of one of their model versions (termed CCM1) in order to familiarize ourselves with a GCM. In June 1991, three ARC employees also spent three days at NCAR in order to learn details of the models and how to run it. The trip was very successful. We are now in electronic communication with them and hope to conduct some preliminary testing for the PNL project in the next few months.

6.0 ADDITIONAL PROGRESS RELEVANT TO REFINING IMPLEMENTATION OF THE SITE CHARACTERIZATION PLAN FOR CLIMATE STUDIES

There were several developments on non-PNL funded activities that are relevant to implementation of the Site Characterization Plan. T. Crowley attended a NATO paleoclimate modeling workshop (May 1991) in France, in which a number of different modeling groups agreed to an intercomparison of model runs for 6000 BP and 18,000 BP. Such intercomparisons enable modelers to test the robustness of their model runs, and are defensible in terms of the Site Characterization Plan because it provides an objective measure as to whether simulations from one model would be representative of climate models as a whole. Furthermore, it was agreed that some modification of observational boundary conditions were required before initiating the intercomparison. This information is valuable for Yucca Mtn. because it may allow for a more accurate simulation of past precipitation variations at Yucca Mtn. T. Crowley will hopefully attend a workshop at which some of the ground rules for the intercomparison will take place, and he also plans to track development of the new data set for initiating model runs. This information will be useful for S. Thompson of NCAR in their validation of their mesoscale model (MM4) run for 18,000 BP. Thompson has also agreed to participate in the intercomparison. The net effect of these efforts is that the Site Characterization Plan will be more defensible in terms of choice of the NCAR GENESIS model and accuracy of our simulation of past climates at Yucca Mtn.

A further development relevant to the Site Characterization Plan occurred on T. Crowley's follow-up visit to the Max Planck Institute (MPI) für Meteorologie in Hamburg, Germany. Although this visit was funded by the institute, Crowley learned while there of an important new series of greenhouse simulations that will in fact be relevant to the Site Characterization Plan. These simulations involved a fully three dimensional coupled ocean-atmosphere GCM, focused on time-varying forcing of CO_2, and

utilized over 3000 hours of time on the Hamburg Cray2 computer. The model results showed variations of the thermohaline circulation in the North Atlantic that has previously been noted in a letter by G. Kukla and identified as a scenario simulation in a draft of the Site Characterization Plan. At the time the draft was written, it was thought that it would not be possible to either simulate or acquire simulations of time-dependent model runs that might actually address this problem. Now, however, through Crowley's serendipitous affiliation with MPI, it seems that it may be possible to acquire the model output from these runs that are relevant to Yucca Mtn. After discussion with S. Thompson, it may even be possible to acquire the regional scale output of the Hamburg model run as input for the MM4. This possibility addresses a major difficulty we had in implementation of the Site Characterization Plan and further strengthens the overall integrity of the Site Characterization Plan. Crowley will track future developments on this matter.

7.0 ARC QUALITY ASSURANCE PROGRAM

7.1 INTRODUCTION

Activity of the ARC Quality Assurance (QA) Program was reduced in Year Four, in concert with technical activities reduction, due to the PNL stop-work order of October 1990 and subsequent budgetary reductions. Despite slow-down of technical activity for a good portion of the year, some QA Administrative activities were maintained throughout, and Software activity was not inconsequential. In this section, we provide a brief summary of Year Three activities and then present our Year Four activities in greater detail.

7.2 YEAR THREE REVIEW

Year Three saw the conclusion of development and testing of the Energy Balance Models (EBMs), while some significant diagnostic routines were produced that will be used throughout the remainder of the project. Eight codes were developed, tested, and implemented for project goals, including one new EBM model and two diagnostic programs. Data base activity expanded to encompass management of some 460 data sets.

Administrative QA activities included training a new scientist and a QA assistant, conducting scheduled Internal Surveillances, and hosting one PNL audit.

7.3 YEAR FOUR ANNUAL SUMMARY

Software Management

QA Procedure Documentation for 14 software programs and 7 software application packages were completed this year. The magnitude of the work is not insubstantial, representing about 1550 pages of procedural documentation and supportive results. Thirteen additional programs were acquired from another ARC

project to provide the results presented in Appendix A. Some of the newer software programs with documentation completed this year are listed in Table B.1. The following is a brief description.

Program SREAD converts the area of snow covered land and ice covered ocean from fraction of global area to 10^6 square kilometers for the Northern and Southern Hemispheres in each of two seasons (postprocessed NEQMOD model output). The program was used extensively in the NEQMOD CO_2 simulations of Appendix D, Third Year Annual Report.

Program MILANK produces the orbital parameters of the Earth) to be input as boundary conditions to certain global climate modeling programs, including the EBMs LINEBM and NEQMOD. MILANK computes the three Earth orbital parameters obliquity, eccentricity, and angle of Winter Solstice from Perihelion based on a coding of the formulations in Berger (1978). The program can produce these parameters for a user-specified year in the past or future, or a time series of these parameters to a specified year into the past or future, with any given time interval. The program was used to produce a single set of parameters for the 128 kyr LINEBM paleosimulation discussed in Appendix I and the 309 kyr time series paleosimulations in Appendix C of the Third Year Annual Report.

Program YUCCA is an interpolation routine specifically designed to extract a time series of Yucca Mtn. temperatures from the LINEBM 309 kyr time series paleosimulations of Appendix C in the Third Year Annual Report. The program makes use of a polynomial interpolation method suitable to the well-behaved temperature gradients generated by LINEBM.

Program ICEMAP was developed to interpolate the University of Maine (UM) group ice sheet model results (see below) to the grid resolutions of our EBMs and the GCMs likely to be encountered in the remainder of the project. The code uses a

TABLE 7.1. QA-Processed Codes for Year Four

Code/Version	Classification	Function
SREAD/1.0	Scientific	Convert NEQMOD snow/ice areas from global fraction to 10^6 sq. kilometers.
MILANK/1.0	Scientific	Compute time series of earth orbital parameters.
YUCCA/1.0	Scientific	Interpolate from LINEBM output temperature field to a point near Yucca Mtn.
ICEMAP/1.0	Scientific	Interpolate UM ice sheet model output to various possible EBM and GCM grids.
StuffIt™/1.6	System	File compression and archival.
Compact Pro™/1.30	System	File compression and archival.
KaleidaGraph™/2.1	System	Graphic data plotting (update of version 2.0).

2-dimensional linear interpolation method appropriate to the ragged gradients of the UM ice sheet height fields. The program may be used to interpolate UM ice sheet model results, both hindcasts and forecasts, to the appropriate GCM grid resolutions should project plans require those fields as input boundary conditions supporting GCM experiments.

Two file compression utilities for the Apple® Macintosh™ were acquired for use with Data Base Management (see below). They are considered System software and use is not documented since execution does not produce reported results. The primary capability of the programs, and their principle purpose to the project, is reduction of required backup disk space (often by as much as 50%). Also, we acquired an update of the commercial graphic data plotting and analysis software KaleidaGraph™ for the Macintosh™.

ARC abandoned the project of improvement of the acquired Low-Resolution General Circulation Model (LRM) of Bette Otto-Bliesner through incorporation of the NCAR CCM1 (Community Climate Model, vers. 1) cloud and radiation routines after budget cutbacks eliminated key personnel. Consequently, QA activities on the improvements were retired this year. However, the LRM in acquired form is under configuration control and available for future experiments.

Data Management

Due to budgetary restrictions earlier in the year, the QA Assistant had to be released. Consequently, staff QA responsibilities have fallen back to the status prior to the third contract year, and the QA Manager has resumed the post of Data Base Steward. Much of the time associated with Stop-Work and restricted budget was spent on Data Base bookkeeping chores, including some reorganization of the project Data Base for greater efficiency of management, access, and recovery.

Select software application output, such as the output from EBM simulations and diagnostic processing, are being consolidated into an Application Archive for more convenient management and access for future work. The collection can easily consume large amounts of data space, so the data are being compressed by one of the acquired system file compression routines.

Year Four data acquisitions included a global surface temperature observations data set from NCAR for the Appendix A work. Additionally, ARC acquired the UM ice sheet model reconstruction of ice age glaciations over the Northern Hemisphere during the Last Glacial Maximum (18,000 yrs. before present).

Administrative Activities

Three senior staff members attended training at NCAR for programmers working with the NCAR GENESIS global climate model. The workshop attendance served as a required QA technical proficiency update on modeling activities for the project near future.

QA Program reviews included regularly scheduled Internal Surveillances, Administrative reviews, and a PNL Audit. Internal Surveillances for the most part have identified backlogged chores, with resolutions that implement a catch-up at the time of surveillance. The items have not impacted reported results. A few findings identify need for procedure revision, which have been postponed as described later. The PNL audit this year identified some minor findings which are to be corrected subject to PNL approval, but the findings do not impact project reported results.

Internal reviews of the QA Program have, over time, revealed some need for select QA Procedure revisions. Some of the revisions are minor, or cosmetic, and some are of more consequence. However, under advise from PNL, most ARC QA Procedure revisions have been put on hold in anticipation of possible review and changes of the PNL QA Program, which might require changes in subcontract QA Programs such as this one.

One of the topics scheduled for revision in the ARC Program concerns software verification requirements of very large and complex codes such as the GCMs of upcoming project work. Our current procedures require test exercises which verify correct coding and execution of the intended numerical design by way of comparison of results with hand calculations, analytic analysis, or with results of a program previously verified under the same procedures. With the models generated by this project, the requirements could be planned and executed throughout the complex code development process. But the procedure presents some special problems for acquired (developed by others) GCM work: the

verification process for 20,000-line atmospheric model code is viewed by ARC as prohibitively expensive and certainly not within the scope of current or future budgets.

Among the proposed solutions under consideration is a revision of procedure to allow a validation experiment to stand in place of verification exercises for such large codes, specifically those that are not developed by ARC. Another method would not rely on procedure revisions, but instead would involve software plans that intentionally deviate from present procedure requirements, such as specifying validation in place of verification. Then we would document the deviation from established procedure in a Deficiency Report, wherein resolution (acceptance of the deviation) approval must come from the project PI and PNL. If we anticipate such verification problems with only a limited number (say, two at most) of GCMs, the later solution has simplification in its favor. A decision on how to proceed will be implemented in Year Five pending the status of the PNL QA Program.

8.0 REFERENCES

Berger, A. 1978. "Long term variations of daily insolations and quaternary climatic changes." J. Atmos. Sci. 35(12):2362-2367.

CLIMAP Project Members. 1981. "Seasonal reconstruction of the earth's surface at the last glacial maximum." Geol. Soc. Amer. Map Chart Ser. MC-36.

Crowley, T. C., G. R. North, and N. R. Smith. 1990. Regional Forecasting with Global Atmospheric Models: Third Year Report. PNL-9416, Pacific Northwest Laboratory, Richland, Washington.

Cubasch, U., K. Hasselmann, H. Höck, E. Maier-Reimer, U. Mikolajewicz, B. D. Santer, and R. Sausen. 1991. "Time-dependent greenhouse warming computations with a coupled ocean-atmosphere model." Nature (submitted).

Hoffert, M. I.,and B. F. Flannery. 1985. "Model projections of the time-dependent response to increasing carbon dioxide." In Projecting the Climatic Effects of Increasing Carbon Dioxide, DOE/ER-0237, edited by M. C. MacCracken and F. M. Luther, U.S. Dept. of Energy, Washington, D.C., pp. 149-190.

Hyde, W. T., T. J. Crowley, K.-Y. Kim, and G. R. North. 1989. "Comparison of GCM and energy balance model simulations of seasonal temperature changes over the past 18,000 years." J. Clim. 2 (8):864-887.

Hyde, W. T., K.-Y. Kim, T. J. Crowley, and G. R. North. 1990. "On the relation between polar continentality and climate: Studies with a nonlinear energy balance model." J. Geophys. Res. 95 (D11):18653-18668.

Manabe, S., K. Bryan, and M. J. Spelman. 1990. "Transient response of a global ocean-atmosphere model to a doubling of atmospheric carbon dioxide." J. Phys. Oceanog. 20 (5):722-749.

Morantine, M. and R. G. Watts. 1990. Upwelling diffusion climate models: Analytical solutions for radiative and upwelling forcing." J. Geophys. Res. 95 (D6):7563-7571.

Schlesinger, M. E. 1988. Physically-Based Modelling and Simulation of Climate and Climatic Change Kluwer, Dordrecht, Netherlands, 1084 pp.

Washington, W. M., and G. A. Meehl. 1989. "Climate sensitivity due to increased CO_2: Experiments with a coupled atmosphere and ocean general circulation model." Clim. Dynam. 4:1-38.

APPENDIX A

SURFACE TEMPERATURE FLUCTUATIONS IN A STOCHASTIC CLIMATE MODEL

by

Kwang-Yul Kim[a]

and

Gerald R. North[b]

[a] Applied Research Corporation, 305 Arguello Drive, College Station, TX 77840

[b] Climate System Research Program, Texas A&M University, College Station, TX 77843

Surface Temperature Fluctuations in a Stochastic Climate Model

Kwang-Yul Kim

Applied Research Corporation, College Station, Texas 77840

and

Gerald R. North

Climate System Research Program, Department of Meteorology
Texas A&M University, College Station, Texas 77843

June, 1991

Revised manuscript submitted to: *Journal of Geophysical Research*

ABSTRACT

This paper considers the geographical distribution of various second moment statistics from a noise-forced energy balance climate model and compares them to the same fields derived from a forty year data set. The variable considered is the surface temperature field over the real globe. The energy balance model is a standardized one used in several previous studies which emphasized the geographical distribution of the seasonal cycle. It treats two dimensional geography explicitly by using a different (uniform) heat capacity over ocean than over land. The study compares the (spatially filtered or 'smoothed') point variance data with those generated by the model in low, medium and high frequency bands. The study also examines the correlation of surface temperature fluctuations at 6 representative test points with those of neighboring points. The only adjustable parameter in the study is the strength of the noise forcing. The intercomparisons show that the model produces maps that look remarkably close to those from the data without too much sensitivity to the form of the driving noise.

1. Introduction

Variability of the surface temperature field is of extreme importance for many reasons. First, we are concerned about the geographical distribution of variance in different frequency bands because we need to be prepared for such variability and we need to understand when an encountered variability is "natural" as opposed to being forced by an external agent. A second reason for studying variance (or in general any second moment quantity of the climate system) in different frequency bands is that it provides an important test of our climate models beyond the usual pedestrian tests such as the geographical distributions of selected monthly averaged snapshots or annual means. A review of how well three general circulation models compute variances for several regions in the United States has recently been given by *Mearns et al.* [1990]. A final reason for studying second moments in various frequency bands is that their characteristics might provide a clue as to the ability of models to predict the correct sensitivity of climate to small externally imposed forcings. This latter is part of a program proposed by *Leith* [1975] and tried in some limited tests by *Bell* [1980, 1985] and discussed in the review by *North et al.* [1981] in connection with noise driven energy balance models (EBMs). In this paper we examine a forty year data set of monthly averaged surface temperature data and attempt to model it with a simple stochastic climate model. As will be revealed the attempt is remarkably successful leading to the likelihood that the model will provide a useful framework for a number of future applications.

Stochastic forcing of energy balance models was suggested many years ago by *Hasselmann* [1977] but he emphasized mainly the slowly responding ocean surface temperature as the computed variable. *Lemke* [1979] used the idea to explore the spectrum for low frequencies with *Budyko's* model [1969]. Some early numerical experiments with a noise forced energy balance model were conducted by *Robock* [1978]. *North et al.* [1981] introduced noise forcing into simple energy balance models with horizontal heat

diffusion. A number of interesting studies have appeared at the global average level where the multiple solution structure and stochastically induced transitions were the main focus [*e.g., Benzi et al.*, 1982]. Most of these studies did not consider that the models could be used in more than a schematic sense. *North and Cahalan* [1982] solved and studied the analytical solutions of a noise forced diffusive model on a uniform planet. The surface temperature $T(\hat{\mathbf{r}}, t)$, ($\hat{\mathbf{r}}$ is a unit vector pointing from the center of the earth to a point on the surface and t is time), satisfied the noise forced damped diffusive equation

$$C\frac{\partial T}{\partial t} - D\nabla^2 T + BT = F$$

where C is a uniform heat capacity per unit area of surface, B is a radiative damping coefficient and D is a thermal diffusion coefficient; $F = F(\hat{\mathbf{r}}, t)$ is a stochastic function which is white in time and whose statistics are rotationally invariant on the sphere

$$\langle F(\hat{\mathbf{r}}, t)F(\hat{\mathbf{r}}', t')\rangle = \sigma_F^2 \rho(\hat{\mathbf{r}} \cdot \hat{\mathbf{r}}')\delta(t - t')$$

where $\langle\cdot\rangle$ denotes ensemble averaging and ρ is the spatial autocorrelation function which depends on the great circle distance or opening angle $\theta = \arccos(\hat{\mathbf{r}} \cdot \hat{\mathbf{r}}')$, separating the two points; σ_F^2 is the total variance of the forcing noise F at a point (this may in general be divergent for white or blue spatial noise but can be rendered finite by use of a cutoff in the spectrum of F). $\delta(\cdot)$ is the Dirac delta function.

By using the spherical harmonics as a basis set, it was found that each mode was dynamically as well as statistically uncoupled, since the spherical harmonics are the eigenfunctions of ∇^2 as well as the Karhunen-Loeve functions for stochastic fields that are statistically rotationally invariant on the sphere. Each mode had an autocorrelation time

$$\tau_n = \frac{\tau_0}{n(n+1)(D/B) + 1}$$

with $\tau_0 = C/B$, and n is the spherical harmonic degree. This solvable model was used by *North and Cahalan* [1982] to investigate the limit of predictability in such stochastic

systems. Later the same system was used by *Leung and North* [1990] to investigate the use of information theory to characterize the decay of information over time following precise knowledge of an initial state. In each of the above cases the noise forced model was used only as a mathematically convenient example, since clearly the fluctuations on planet earth are not statistically rotationally invariant on the sphere and the case for linear diffusive heat transport is not compelling.

Two recent studies have suggested that the noise forced EBM may be a useful model for actual quantitative studies with the real atmospheric system. *Leung and North* [1991] have shown that the noise forced EBM can be used to fit the surface temperature fluctuation data from a long GCM run of the atmosphere of an all land planet with no topography or seasons and no zonal symmetry breaking features. That the diffusion and heat capacity parameters, D and C, estimated from the objective fitting procedure were very close to the values found in fitting observed data for the seasonal cycle of the planet with geography [*North et al.*, 1983; *Hyde et al.*, 1989] gave reason to believe that the model is able to generate reasonable correlation structures in space and time and that these are brought about by the same diffusion and heat capacity parameters needed to fit the earth's forced seasonal cycle. A second study using the same general circulation model (the CCM0) [*North et al.*, 1991] reinforced the finding by showing that the ensemble average of the GCM surface temperature when forced responded in an essentially linear manner.

In this paper we examine natural fluctuations of the surface temperature using forty years (1940–1980) of monthly averaged data (the United Kingdom data stored in the NCAR archives; we converted it from a 72×36 grid to a spherical harmonic expansion truncated triangularly at degree 11). We looked at several measures of the fluctuations: 1) The temporal spectrum of the global average variations. 2) Maps of the variance contained in three interesting frequency bands. 3) The spatial correlations of the temperature field at selected test points with that of neighboring points so that

correlation contours could be constructed around the test points. These latter were also examined separately for fluctuations contained in the same interesting frequency bands. Next we used the EBM studied and standardized by *North et al.* [1983] without change of any parameters and forced it with white noise in both space and time. The only new parameter introduced was the overall strength of the noise forcing.

After a mathematical introduction to the techniques employed, we present the results mostly in the form of maps that are easily interpreted.

2. Model and Procedures

The linear energy balance equation [*North et al.*, 1983; *Hyde et al.*, 1989] is given by

$$C(\hat{\mathbf{r}})\frac{\partial T(\hat{\mathbf{r}},t)}{\partial t} + A + BT(\hat{\mathbf{r}},t) - \nabla\cdot(D(x)\nabla T(\hat{\mathbf{r}},t)) = Q\,S_{\odot}(\hat{\mathbf{r}},t)a(\hat{\mathbf{r}}) + F(\hat{\mathbf{r}},t), \quad (1)$$

where $\hat{\mathbf{r}} = (\theta,\phi)$ is a point on the Earth's surface; $x = \sin\theta$ is the sine of latitude; $C(\hat{\mathbf{r}})$ is the local heat capacity per unit area [it takes on different constant values for ocean, land and perennial sea ice]; $D(x) = D_0(1+D_2x^2+D_4x^4)$ is the local diffusion coefficient [$D_0/(BR_0^2)$ is dimensionless; R_0=earth radius]; $T(\hat{\mathbf{r}},t)$ is the temperature field to be solved for; $S_{\odot}(\hat{\mathbf{r}},t)$ is the normalized distribution of seasonal radiation reaching the top of the atmosphere; Q is the solar constant divided by 4; $a(\hat{\mathbf{r}})$ is the coalbedo; $F(\hat{\mathbf{r}},t)$ is the noise forcing function; A and B are the parameters of the best linear fit for the infrared emission to space. Values of the parameters used in this study are presented in Table 1. Since (1) is linear, the anomaly of the response $T' = T - T_0$ due to the noise forcing F is governed by

$$C(\hat{\mathbf{r}})\frac{\partial T'(\hat{\mathbf{r}},t)}{\partial t} + BT'(\hat{\mathbf{r}},t) - \nabla\cdot(D(x)\nabla T'(\hat{\mathbf{r}},t)) = F(\hat{\mathbf{r}},t) \quad (2)$$

where $T_0(\hat{\mathbf{r}},t)$ is the ensemble averaged seasonal cycle. The details about the noise forcing will be discussed later. For the sake of convenience, we will drop the prime for

T. We may expand the space dependent functions into spherical harmonics (complex valued, orthonormal, *Arfken*, 1985):

$$
\begin{aligned}
C(\hat{\mathbf{r}}) &= \sum_j \sum_k C_{jk} Y_j^k(\hat{\mathbf{r}}); \\
D(x) &= \sum_j D_j Y_j^0(\hat{\mathbf{r}}); \\
T(\hat{\mathbf{r}},t) &= \int_{-\infty}^{\infty} df \sum_l \sum_m T_{lm}^f Y_l^m(\hat{\mathbf{r}}) e^{2\pi i f t}; \\
F(\hat{\mathbf{r}},t) &= \int_{-\infty}^{\infty} df \sum_l \sum_m F_{lm}^f Y_l^m(\hat{\mathbf{r}}) e^{2\pi i f t}.
\end{aligned} \tag{3}
$$

Table 1: Model Parameters

Symbol	Value	Reference
B	2.094 W/m^2/°C	*North et al.* [1983]
C_W/B	4.6 yrs; Ocean heat capacity/area	*North et al.* [1983]
C_I	$C_W/6.5$; Sea-ice heat capacity/area	*North et al.* [1983]
C_L	$C_W/60$; Land heat capacity/area	*North et al.* [1983]
D_0/B	0.39 m	*North et al.* [1983]
D_2	-1.33	*North et al.* [1983]
D_4	0.67	*North et al.* [1983]
$\sqrt{\langle \lvert F_{lm}^f \rvert^2 \rangle}$	1.00 (W/m^2) yr	present study

After multiplying by Y_p^q to project the (p,q) component and using a summation convention on the repeated indices we find

$$
\begin{aligned}
&2\pi i f C_{jk} T_{lm}^f \int Y_j^k Y_l^m Y_p^{-q}\, d\Omega + B T_{lm}^f \int Y_l^m Y_p^{-q}\, d\Omega \\
&\quad + \frac{1}{2}\left(p(p+1) + l(l+1) - j(j+1)\right) D_j T_{lm}^f \int Y_j^0 Y_l^m Y_p^{-q}\, d\Omega \\
&\qquad\qquad = F_{lm}^f \int Y_l^m Y_p^{-q}\, d\Omega,
\end{aligned} \tag{4}
$$

where the integration is over the whole globe. In the last equation and in what follows we adopt a summation convention which implies triangular truncation at a specified degree L: $\sum_{l=0}^{L}\sum_{m=-l}^{l}(\cdot)_{lm}$. Summation will always be implied when indices are repeated unless explicitly indicated otherwise.

Since (2) is linear with time independent coefficients, (4) is separable for each frequency f. For each f, (4) may be rewritten schematically as

$$A^f T^f = F^f, \tag{5}$$

where A^f is the coefficient matrix, T^f is the temperature response vector, and F^f is the forcing vector, all depending on the frequency f.

Using (3) and (5), the time series of the temperature response is given by

$$\int T^f_{lm} Y_l^m(\hat{\mathbf{r}}) e^{2\pi i f t}\, dt = \int T^f_i Y_i(\hat{\mathbf{r}}) e^{2\pi i f t}\, dt = \int B^f_{ij} F^f_j Y_i(\hat{\mathbf{r}}) e^{2\pi i f t}\, dt, \tag{6}$$

where $B = A^{-1}$, and $i = i(l,m)$ and $j = j(l',m')$ are one-to-one functions of order l and rank m. The variance of the temperature response contained in the frequency band Δf then is

$$\begin{aligned}\mathrm{Var}(T(\hat{\mathbf{r}},t)) &= \left\langle \int_{f\in\Delta f} T^f_i Y_i(\hat{\mathbf{r}}) e^{2\pi i f t}\, df \left(\int_{f'\in\Delta f} T^{f'}_j Y_j(\hat{\mathbf{r}}) e^{2\pi i f' t}\, df' \right)^* \right\rangle \\ &= \int_{f\in\Delta f}\int_{f'\in\Delta f} \langle (T^f_i)(T^{f'}_j)^* \rangle\, Y_i(\hat{\mathbf{r}}) Y_j^*(\hat{\mathbf{r}})\, e^{2\pi i (f-f')t}\, df\, df'\end{aligned}$$

where * denotes complex conjugation. Because the time series are stationary we have

$$S^T_{ij}(f)\delta(f-f') \equiv \langle (T^f_i)(T^{f'}_j)^* \rangle$$

where $S^T_{ij}(f)$ is the cross-spectral density of T between the spatial components i and j at frequency f. Note that from (6) it follows that

$$\begin{aligned} S^T_{ij}(f) &= (B^f_{ik})(B^f_{jl})^* S^F_{kl}(f) \\ &= (B^f_{ik})(B^f_{jl})^* S^F(f)\delta_{kl}\end{aligned}$$

where $S^F_{kl}(f)$ is the cross-spectral density of the forcing noise. The last property holds only if the driving noise is rotationally invariant on the sphere. We will make this simplifying assumption throughout what follows. The point variance of $F(\hat{\mathbf{r}},t)$ may be written explicitly

$$\begin{aligned}\langle F^2(\hat{\mathbf{r}},t)\rangle &= \int_{-f_c}^{f_c} df \sum_{l=0}^{L}\sum_{m=-l}^{l} \langle |F^f_{lm}|^2\rangle \, |Y_l^m(\hat{\mathbf{r}})|^2 \\ &= \int_{-f_c}^{f_c} df \sum_{l=0}^{L} \frac{2l+1}{4\pi}\langle |F^f_{lm}|^2\rangle,\end{aligned}$$

where in the last step $\langle |F^f_{lm}|^2\rangle$ is considered to be constant. Note that f_c and L are cutoffs in the otherwise flat noise spectrum. The scale of the components $\sqrt{\langle |F^f_{lm}|^2\rangle}$ required to fit the temperature variance data (Table 1) is $\sim 1.00\ (\mathrm{W/m^2})\,\mathrm{yr}$.

Finally, we may write the variance of the surface temperature in the frequency band Δf as

$$\mathrm{Var}(T(\hat{\mathbf{r}},t))_{\Delta f} = \int_{f\in\Delta f} G^f_{ij} Y_i(\hat{\mathbf{r}}) Y_j^*(\hat{\mathbf{r}})\, df$$

where we have defined a covariance matrix of the response field

$$G^f_{ij} = (B^f_{ik}) S^F(f) (B^f_{jk})^*. \tag{7}$$

From (6), the covariance in the frequency band Δf between the fluctuations at two separated points $\hat{\mathbf{r}}_1$ and $\hat{\mathbf{r}}_2$ can be written as

$$\mathrm{Cov}(T(\hat{\mathbf{r}}_1,t), T(\hat{\mathbf{r}}_2,t))_{\Delta f} = \int_{f\in\Delta f} G^f_{ij} Y_i(\hat{\mathbf{r}}_1) Y_j^*(\hat{\mathbf{r}}_2)\, df.$$

The spatial correlation coefficient, then, is given by

$$\mathrm{Corr}(T(\hat{\mathbf{r}}_1,t), T(\hat{\mathbf{r}}_2,t))_{\Delta f} = \frac{|\mathrm{Cov}(T(\hat{\mathbf{r}}_1,t), T(\hat{\mathbf{r}}_2,t))_{\Delta f}|}{\sqrt{\mathrm{Var}(T(\hat{\mathbf{r}}_1,t))_{\Delta f}\,\mathrm{Var}(T(\hat{\mathbf{r}}_2,t))_{\Delta f}}}.$$

Similarly, the temporal covariance with a lag Δt is defined by

$$\begin{aligned}
&\mathrm{Cov}(T(\hat{\mathbf{r}},t),T(\hat{\mathbf{r}},t+\Delta t))_{\Delta f} \\
&\qquad = \langle \int_{f\in\Delta f} T_i^f Y_i(\hat{\mathbf{r}}) e^{2\pi i f t}\, df \Big(\int_{f'\in\Delta f} T_j^f Y_j(\hat{\mathbf{r}}) e^{2\pi i f'(t+\Delta t)}\, df' \Big)^* \rangle \\
&\qquad = \int_{f\in\Delta f} e^{2\pi i f \Delta t} \langle (T_i^f)(T_j^f)^* \rangle Y_i(\hat{\mathbf{r}}) Y_j^*(\hat{\mathbf{r}})\, df \\
&\qquad = \int_{f\in\Delta f} e^{2\pi i f \Delta t} G_{ij}^f Y_i(\hat{\mathbf{r}}) Y_j^*(\hat{\mathbf{r}})\, df
\end{aligned}$$

and hence the temporal correlation is defined by

$$\mathrm{Corr}(T(\hat{\mathbf{r}},t),T(\hat{\mathbf{r}},t+\Delta t))_{\Delta f} = \frac{|\mathrm{Cov}(T(\hat{\mathbf{r}},t),T(\hat{\mathbf{r}},t+\Delta t))_{\Delta f}|}{\mathrm{Var}(T(\hat{\mathbf{r}},t))_{\Delta f}}.$$

The actual computation of the covariance matrix, (7), is carried out for a series of discrete frequencies in the band Δf with the integrations approximated by the Trapezoidal rule. It was found that the covariance matrix is a very smooth function of the frequency. Less than 25 harmonics were sufficient to accurately describe the response characteristics in the 1 month – 10 year band.

For comparisons, similar statistics were computed for the observational data. It was assumed that the observational data consist mainly of the response to the annual insolation forcing and partly to the noise response due to dynamic instabilities, changing boundary conditions, etc. The response to the annual forcing was crudely removed by subtracting monthly means from their respective months. In other words, an annual cycle and its harmonics were removed. The data set consists of forty years of monthly averaged observations on a 72×36 uniform grid with virtually no preprocessing obtained from the NCAR archives. For a consistent comparison with the EBM, the observational data were smoothed to the same level via an order 11 triangular truncation employing a spherical harmonic basis set. Note also that the observational data set is not really long enough for true ensemble averages of the desired statistics. For the present purposes we assumed the raw statistics to be not very different from their ensemble averages.

The Fourier expansion coefficients T^f of the observational data were obtained by performing a Fourier transformation in time:

$$T^f(\hat{\mathbf{r}}) = \int_{-\infty}^{\infty} T(\hat{\mathbf{r}}, t) e^{-2\pi i f t}\, dt.$$

The power spectral density function at a specific point $\hat{\mathbf{r}}$ is a plot of $|T^f(\hat{\mathbf{r}})|^2$ vs. f with a proper normalization factor. The normalization factor is such that the area under the spectral curve becomes the total variance. All other computations with the data were with standard techniques [*Newton,* 1988].

3. Results and Discussion

Given a forcing spectrum, $S^F(f)$, the linear energy balance model (2) can be solved for the covariance matrices defined in (7) for a selected frequency f. From the covariance matrices, various response characteristics of the linear EBM can be derived — variance distribution in space and time, correlation time scale, spatial scale of correlation, etc. The single adjustable parameter in the study is the amplitude of the noise forcing $\sqrt{\langle |F^f_{lm}|^2 \rangle} = A_F;\ -f_c \le f \le f_c$. We adjusted this amplitude until the point (smeared by our spatial filter, of course) temperature variance was approximately in agreement with that of the correspondingly filtered data (cf., Table 1). We chose a point in Middle Asia for the matching since that is the location of largest variance in both model and data in all frequency bands. After this calibration has been accomplished once and for all, we need only examine the results.

a. Spectrum of the global response

Figure 1 compares the spectral density of the global-average temperature of the observations and those of the energy balance model. Because the response spectrum of the observations based on the only one 40 year realization was rather ragged, an auto-regressive fitting of order 5 was plotted instead [*Newton,* 1988]. The best order

for auto-regressive fitting was determined by the CAT (criterion autoregressive transfer function) criterion [cf., *Newton,* 1988]. Both the observational and model spectra are slightly red as expected. We find this fit to be even better than we would have expected, but note the departure at very low frequencies (<1/(5 yrs)). The data indicate less variance for multiyear periods than the model. This is most likely due to our omission of the deep ocean. We intend to address this issue of deep ocean contributions to the surface variablility in a future paper.

b. Variance distributions

Figures 2–4 are the contour maps of the variance of the observed temperature and of the response of the linear EBM. The resemblance between the geography of the land and the ocean and the distribution of variance contained in the frequency band $\Delta f = \{f : 0.1/\text{yr} \leq f \leq 6/\text{yr}\}$, is very remarkable both in the observations and in the model. Agreement between the observations and the model is also apparent in the variance contained in the 2 month – 1 year period band. We have shaded areas on the maps where data is insufficient to compute the variance (see each figure caption). The lack of consistency over Antarctica may be due to topographical influences not in the model and/or the sparcity of data over the area.

A rough idea of the sampling error can be obtained assuming the statisitics are Gaussian. Since the autocorrelation time over Middle Asia is about a month (see later discussion) and we are considering 480 months of data, we might consider that there are roughly 240 independent samples or degrees of freedom. Such a sum of squared Gaussian variates is distributed as a χ^2 variate with 240 degrees of freedom. The standard error for the variance is $2\sigma_T^2/\sqrt{240}$, which is only of order of 12 percent of the temperature variance itself. For the present purposes this is considered sufficiently accurate. Over oceans the standard error for the temperature variance are of course much larger because of the longer autocorrelation times (cf., Fig. 7).

Although the geographic pattern of the variance in the 1 – 5 year band (Fig. 4) is similar to that in Fig. 3, there is one major difference, *i.e.*, the large variance at the eastern equatorial Pacific in the observation data. This pattern of variability is clearly associated with El Niño. Since the simple EBM does not include this effect, the discrepancy is to be expected. On the other hand, we learn that the effect of El Niño constitutes virtually all of the unexplained variance of surface temperature for time scales greater than a year.

As the temporal scale becomes larger, the distinction between the land and the ocean becomes weaker. Model variance in lower frequency bands becomes more uniform (not shown) exhibiting less distortion due to the size and placement of the land masses. The variance within the same band in the observations shows slightly more dependence on the geography of the land masses than does the model at low frequencies. Treatment of the lower frequencies will require inclusion of deep ocean effects in the noise forced model.

c. Spatial correlation

Figures 5 and 6 are the maps of the spatial correlation at selected test points. The heavy contours represent the $1/e$ value of the correlation for reference. Before the details, some of the general patterns of the spatial correlation are summarized in the following: i) The spatial correlation scale of the interannual variability is in the range of 1500-2000 km. This is consistent with the EBM low frequency diffusive length scale $\sqrt{D/B}$ [cf. *North,* 1984; *Hansen and Lebedeff*, 1987; *North et al.*, 1991]. The corresponding length scale is shorter for higher frequency temporal fluctuations [*North et al.,* 1983b]. ii) The spatial correlation length scale is larger over the land than over the ocean. A comparison of the spatial correlation functions of the observations shows that the correlation length scale over large continental interiors is larger than that over the ocean. This is because the very definition of high versus low frequency depends on

the relevant relaxation time of the surface medium. It is about one month over land and about 5 years over the open ocean. Note also that at (120°W , 40°N), a coastal point, the correlation length scale is longer toward the continent than toward the ocean. iii) As shown in Figs. 5 and 6, the spatial correlation length scale increases upon averaging the field over longer times. In the model this simply expresses the lengthening of the length scale toward its low frequency limit $\sqrt{D/B}$. Note that a similar dependency is apparent in the data except for the obvious interference by El Niño.

A comparison of the observations and model in their spatial correlations of the intra-annual variability (Fig. 5) is quite favorable. Over the land, the model spatial correlation scale with the white noise forcing is quite comparable to that of the observations. Bear in mind that the model ocean is mixed instantaneously from the top to the bottom of the mixed layer. In other words, the model correlation scale is for the entire column of the mixed layer, while that of the observations is for the surface temperature field.

A large discrepancy in the spatial correlation of the 1 year to 10 year variability is found over the eastern equatorial Pacific. As alluded to earlier, this large spatial correlation is surely tied to El Niño. As the temporal scale becomes larger, the spatial correlation scale of the observed temperature field becomes larger but highly anisotropically. As mentioned above, the model correlation scale over the ocean is for the entire column of the mixed layer while that for the observation is for the surface temperature field.

d. Temporal correlation

Temporal correlation is another measure of the sensitivity of a model as well as an important consideration for sampling. Figure 7 shows the contour plots of the relaxation time for the observation and the model. A spatial moving average (50° × 25° box) was passed over the resulting map to remove noisy fine structure and to facilitate visual

interpretation. The essential content was not altered by the smoothing. It is consistent both in the model and in the observations that the correlation time scale is shorter over the land than over the ocean. Note that the model temporal scale is C/B which is about one month for an all-land planet and 4.5 years for an all-ocean planet. It is clear that the distribution of land mass is an important factor controlling the correlation time scale of the response.

Two rather large discrepancies are at the eastern equatorial Pacific and at the Antarctic circumpolar current region. The former is clearly associated with El Niño. The latter deviation may be due to the inadequacy of the observational data.

e. Blue noise forcing

In addition to the above experiments we conducted a number of experiments with a form of the noise forcing that could be characterized as "blue" in space. We increased the forcing variance linearly by spherical harmonic degree while keeping it white in time. This was motivated by the study by *Leung and North* [1991] who found that in fitting the noise forced EBM to a long GCM run, a slightly better fit could be obtained using this blue spatial noise. The underlying reason for the improved fit was the likelihood that the instabilities in the atmosphere which presumably give rise to the noise are concentrated more at the higher wave numbers which are most unstable in atmospheric flows. We repeated all of the above experiments with the blue noise forcing (still white in time) and generated the corresponding maps. We found that in some cases there was an improvement but not sufficient to present here and not sufficient to justify the addition of another free parameter describing the "slope" of the blue noise spectrum for most applications.

4. Concluding Remarks

This study has shown that noise forced energy balance models can produce the main characteristics of second moment fields of the surface temperature in both space

and time. It is remarkable that dynamical and even topographical considerations play almost no role in the maps shown. The only exceptions are the phenomena clearly associated with El Niño and other low frequency oceanic upwelling processes.

We feel that the findings are important for a number of future applications. 1) The errors made by using a finite number of thermometers over the planet to estimate a global average can now be assessed with some reliability using a relatively simple stochastic climate model combined with standard estimation methodology [*e.g., North and Nakamoto,* 1989]. Using the correlation lengths as a guide in thermometer spacing on the globe has already been convincingly argued by *Hansen and Lebedeff* [1987]. Our results will allow quantitative assessment of the errors made in detecting climate change with the historically sparse network. These findings can in turn help in developing optimal estimation or detection strategies [*e.g., Bell,* 1982]. 2) Now that a simple model has been shown to be this useful, we can begin to think more seriously about its use in predictability [*North and Cahalan,* 1982; *Leung and North,* 1990] and transient climate studies [*North et al.,* 1983b]. These latter experiments must continually be compared with similar studies with general circulation models. This interactive hierarchical approach should prove useful in providing badly needed insight into a number of climate change problems. 3) We hope the findings of our study will also point to the possibility of eventually using natural fluctuation statistics in narrowing the uncertainties in our very best fully coupled GCMs.

Acknowledgements

We are grateful for support from the DOE *Quantitative Links* Program (Texas A&M) and from a contract (ARC) from the Pacific Northwest Laboratory operated by Battelle Memorial Institute under contract DE-AC06-76RLO 1830. We have benefitted from many discussions with T. J. Crowley.

References

Arfken, G., *Mathematical Methods for Physicists*, 3rd Ed., Academic Press, 985pp., 1985.

Bell, T. L., Climate sensitivity from fluctuation dissipation: Some simple model tests, *J. Atmos. Sci.*, *37*, 1701–1707, 1980.

Bell, T. L., Optimal weighting of data to detect climatic change: Application to the carbon dioxide problem, *J. Geophys. Res.*, *87*, 11,161–11,170, 1982.

Bell, T. L., Climate sensitivity and fluctuation-dissipation relations, in *Turbulence and Predictability in Geophysical Fluid Dynamics and Climate Dynamics*, Soc. Italiana di Fisica, 424–440, 1985.

Benzi, R., G. Parisi, A. Autera, and A. Vulpaiani, Stochastic resonance in climatic change, *Tellus*, *34*, 820–829, 1985.

Budyko, M. I., The effect of solar radiation variations on the climate of hte earth, *Tellus*, *21*, 611–619, 1969.

Hansen, J., and S. Lebedeff, Global trends of meassured surface air temperature, *J. Geophys. Res.*, *92*, 13,345–13,372, 1987.

Hasselmann, K., Stochastic climate models, Part I: Theory, *Tellus*, *28*, 473–484, 1976.

Hyde, W., T. J. Crowley, K. Y. Kim, and G. R. North, Comparison of GCM and energy balance model simulations of seasonal temperature schanges over the past 18000 years, *J. Clim.*, *2*, 864–887, 1989.

Lemke, P., Stochastic climate models, Part 3: Application to zonally averaged energy models, *Tellus*, *29*, 385–392, 1979.

Leung, L., and G. North, Information theory and climate prediction, *J. Clim.*, *3*, 5–14, 1990.

Leung, L., and G. North, Atmospheric variability on a zonally symmetric all land planet, *J. Climate*, *accepted for publication*, 1991.

Mearns, L. O., S. H. Schneider, S. L. Thompson, and L. R. McDaniel, Analysis of climatic variability in GCMs: comparison with observations and chanes in $2 \times CO_2$ experiments, *J. Geophys. Res.*, *95*, 20,469–20,490, 1990.

Newton, H. J., *TIMESLAB: A Times Series Analysis Laboratory*, Wadsworth and Brooks, 623pp., 1988.

North, G., The small ice cap instability in diffusive climate models, *J. Atmos. Sci.*, *41*, 3390–3395, 1984.

North, G., and R. Cahalan, Predictability in a solvable stochastic climate model, *J. Atmos. Sci.*, *38*, 504–513, 1982.

North, G. R., R. F. Cahalan, and J. A. Coakley, Energy balance climate models, *Rev. Geophys. Space Phys.*, *19*, 91–121, 1981.

North, G., J. Mengel, and D. Short, Simple energy balance model resolving the seasons and the continents: Application to the astronomical theory of the ice ages, *J. Geophys. Res.*, *88*, 6576–6586, 1983a.

North, G., J. Mengel, and D. Short, On the transient response patterns of climat to time dependent concentrations of atmospheric CO_2, in *Climate Processes and Climate Sensitivity*, Geophysical Monograph 29, Maurice Ewing, Vol. 5, 164–170, 1983b.

North, G., and S. Nakamoto, Formalism for comparing rain estimation designs, *J. Atmos. and Oceanic Technol.*, *6*, 985–992, 1989.

North, G., K. Yip, L. Leung, and R. Chervin, Forced and free variations of the surface temperature field. *J. Clim.*, *submitted*, 1991.

Robock, A., Internally and externally caused climate change, *J. Atmos. Sci.*, *35*, 1111–1122, 1978.

Figure Legends

Figure

1. Spectral density functions of the global average temperatures: thick line - observation (auto-regressive fitting of order 5); thin line with circle - linear energy balance model response to a noise forcing white in space and time.
2. Geography of the distribution of variance ($°C^2$) within 2 month – 10 year band: a) observations (shaded areas indicate regions with less than 30 years of data available); b) linear energy balance model with a noise forcing white in space and time.
3. Geography of the distribution of variance within 2 month – 1 year band: a) observations (shaded areas indicate regions with less than 10 years of data available); b) linear energy balance model with a noise forcing white in space and time.
4. Geography of the distribution of variance within 1 – 5 year band: a) observations (shaded areas indicate regions with less than 30 years of data available); b) linear energy balance model with a noise forcing white in space and time.
5. Spatial correlations of fluctuations within 2 month – 1 year band at six selected sampling points: a) observations (shaded areas indicate regions with less than 10 years of data available); b) linear energy balance model with a noise forcing white in space and time. The test points are (30°W, 50°N), (90°E, 50°N), (120°W, 40°N), (10°E, 20°N), (150°W, 0°N), (0°E, 90°S).
6. Spatial correlations of fluctuations within 1 year – 10 year band (annual average temperature field) at selected sampling points: a) observations (shaded areas indicate regions with less than 30 years of data available); b) linear energy balance model with a noise forcing white in space and time.
7. Correlation time scale (defined as the $1/e$ point of decay) of the response within 2 month - 10 year band: a) observation (moving averaged over a 50° × 25° box;

shaded areas indicate regions with less than 30 years of data available); b) linear energy balance model with a noise forcing white in space and time.

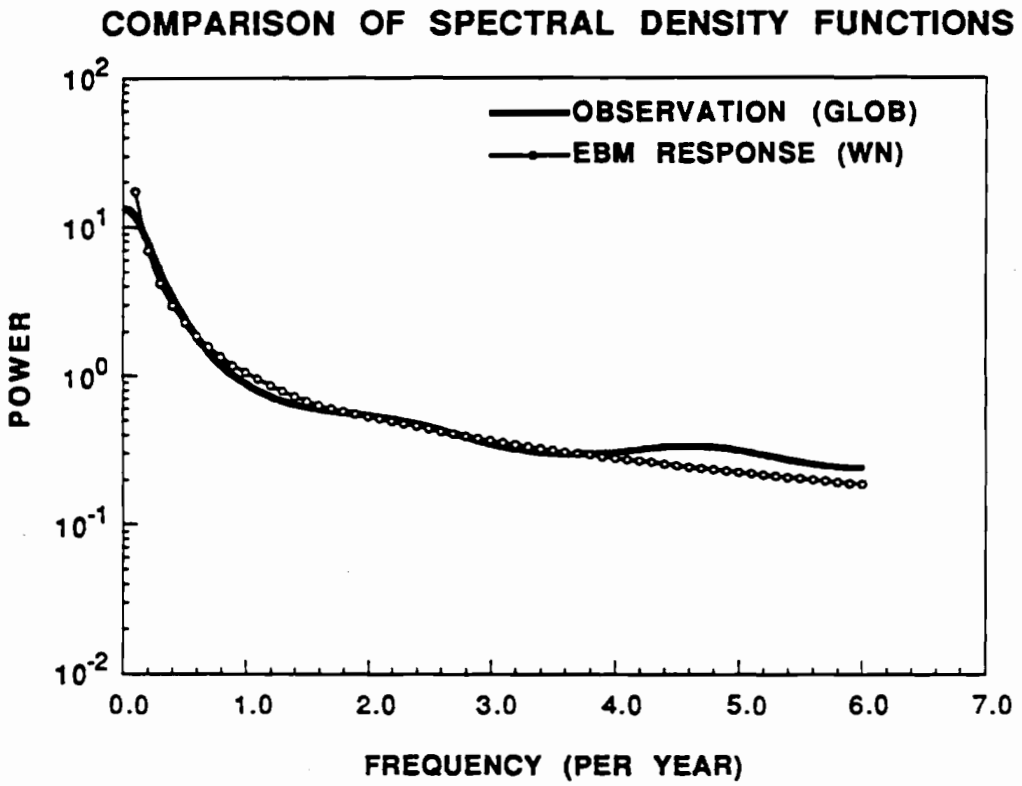

Fig. 1. Spectral density functions of the global average temperatures: thick line - observation (auto-regressive fitting of order 5); thin line with circle - linear energy balance model response to a noise forcing white in space and time.

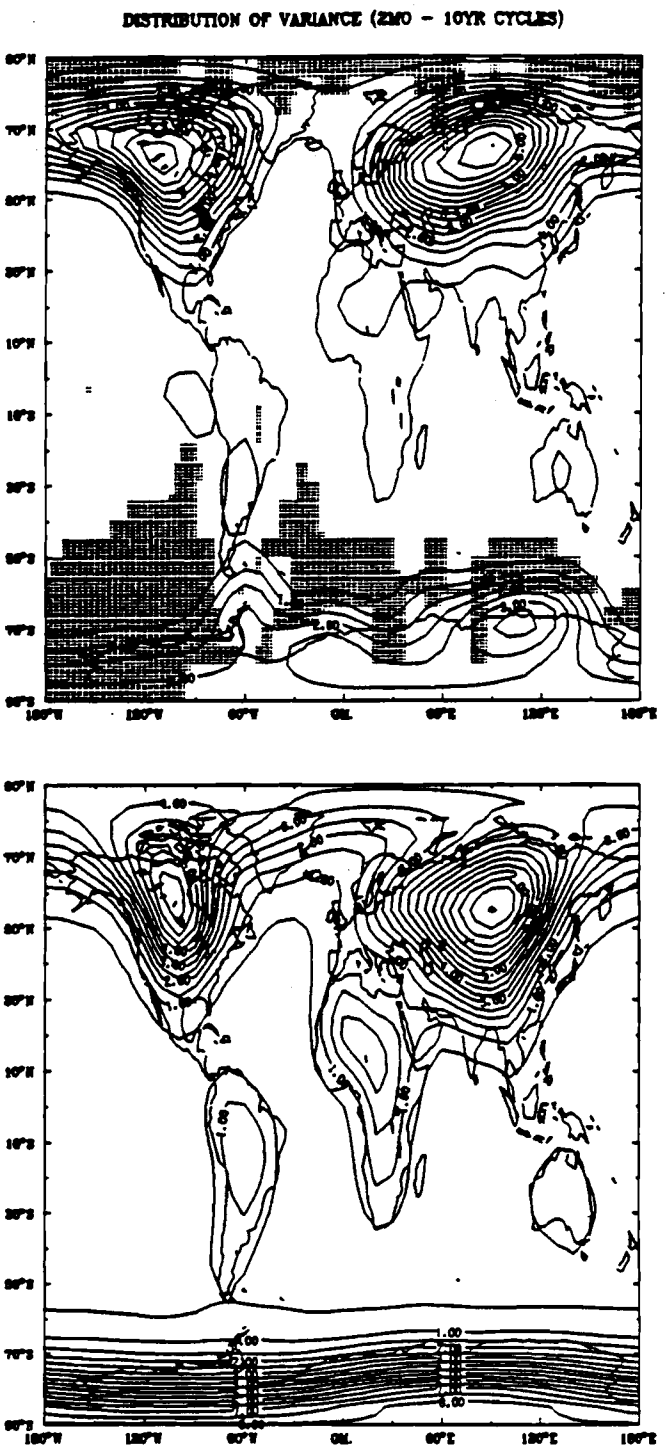

Fig. 2. Geography of the distribution of variance ($°C^2$) within 2 month – 10 year band: a) observations (shaded areas indicate regions with less than 30 years of data available); b) linear energy balance model with a noise forcing white in space and time.

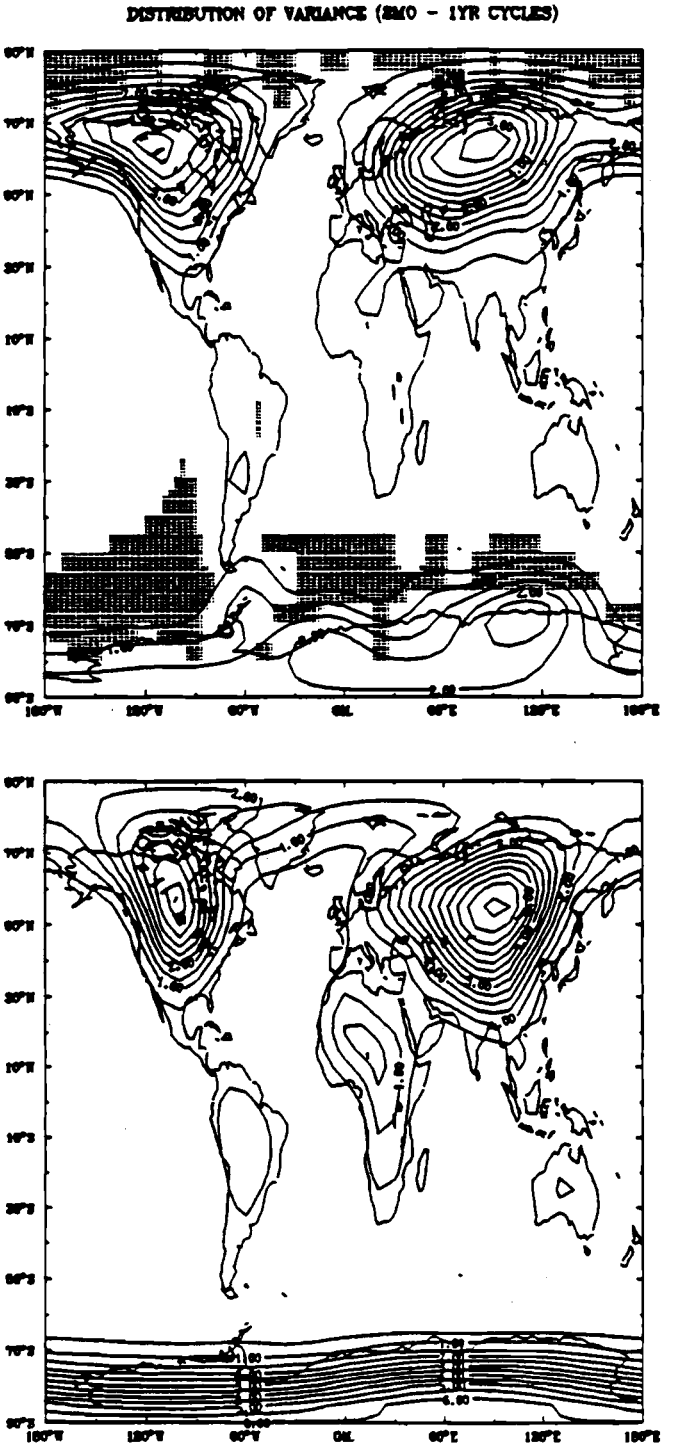

Fig. 3. Geography of the distribution of variance within 2 month – 1 year band: a) observations (shaded areas indicate regions with less than 10 years of data available); b) linear energy balance model with a noise forcing white in space and time.

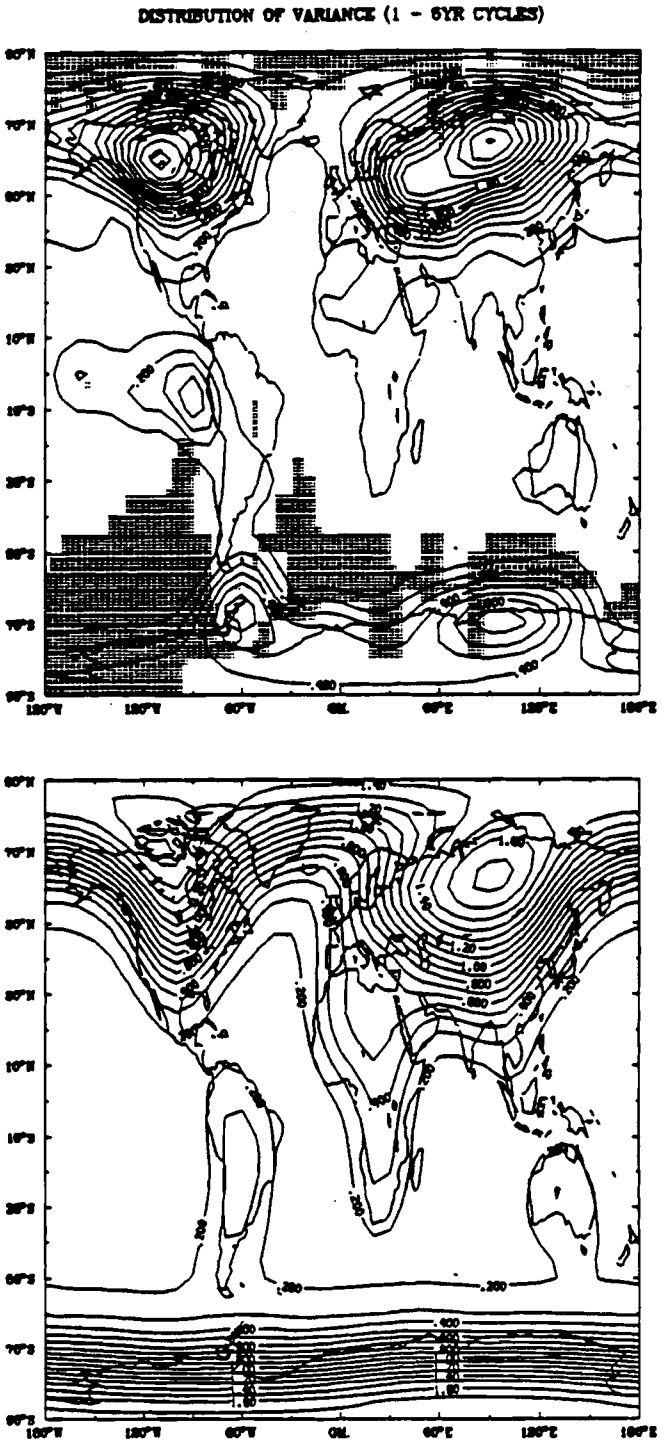

Fig. 4. Geography of the distribution of variance within 1 – 5 year band: a) observations (shaded areas indicate regions with less than 30 years of data available); b) linear energy balance model with a noise forcing white in space and time.

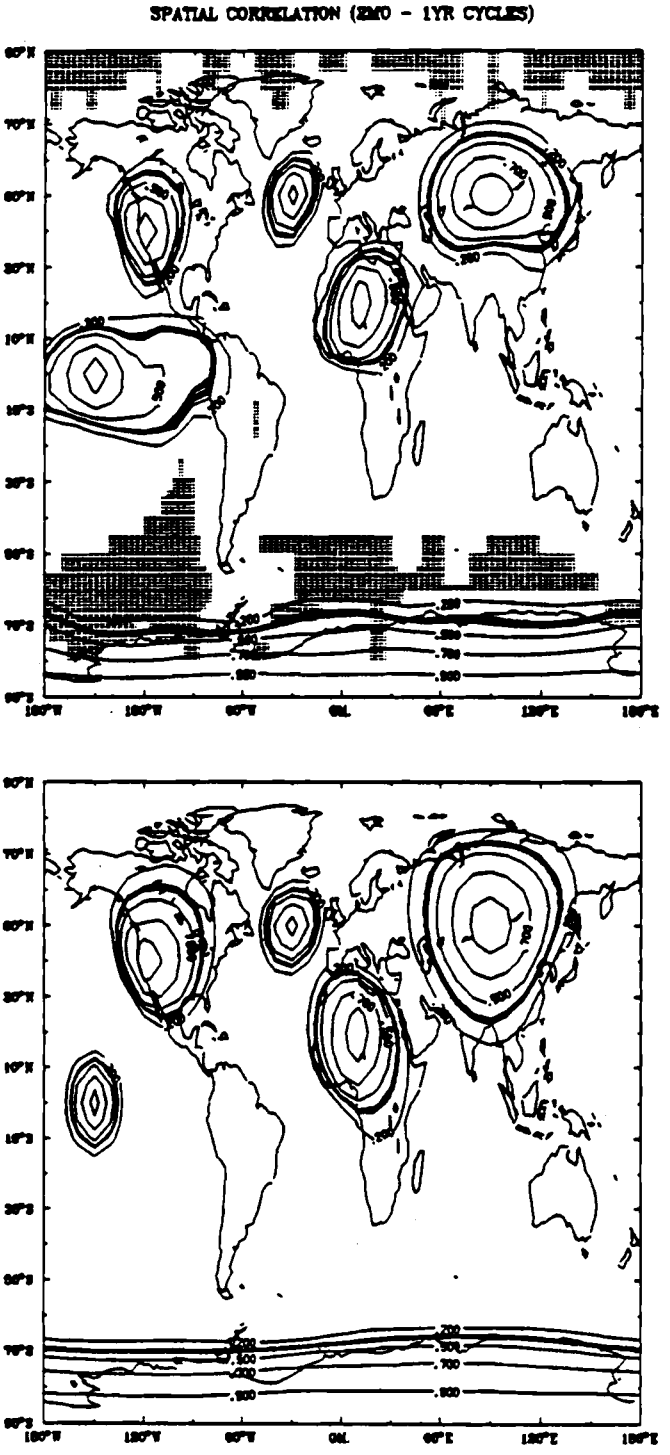

Fig. 5. Spatial correlations of fluctuations within 2 month – 1 year band at six selected sampling points: a) observations (shaded areas indicate regions with less than 10 years of data available); b) linear energy balance model with a noise forcing white in space and time. The test points are (30°W, 50°N), (90°E, 50°N), (120°W, 40°N), (10°E, 20°N), (150°W, 0°N), (0°E, 90°S).

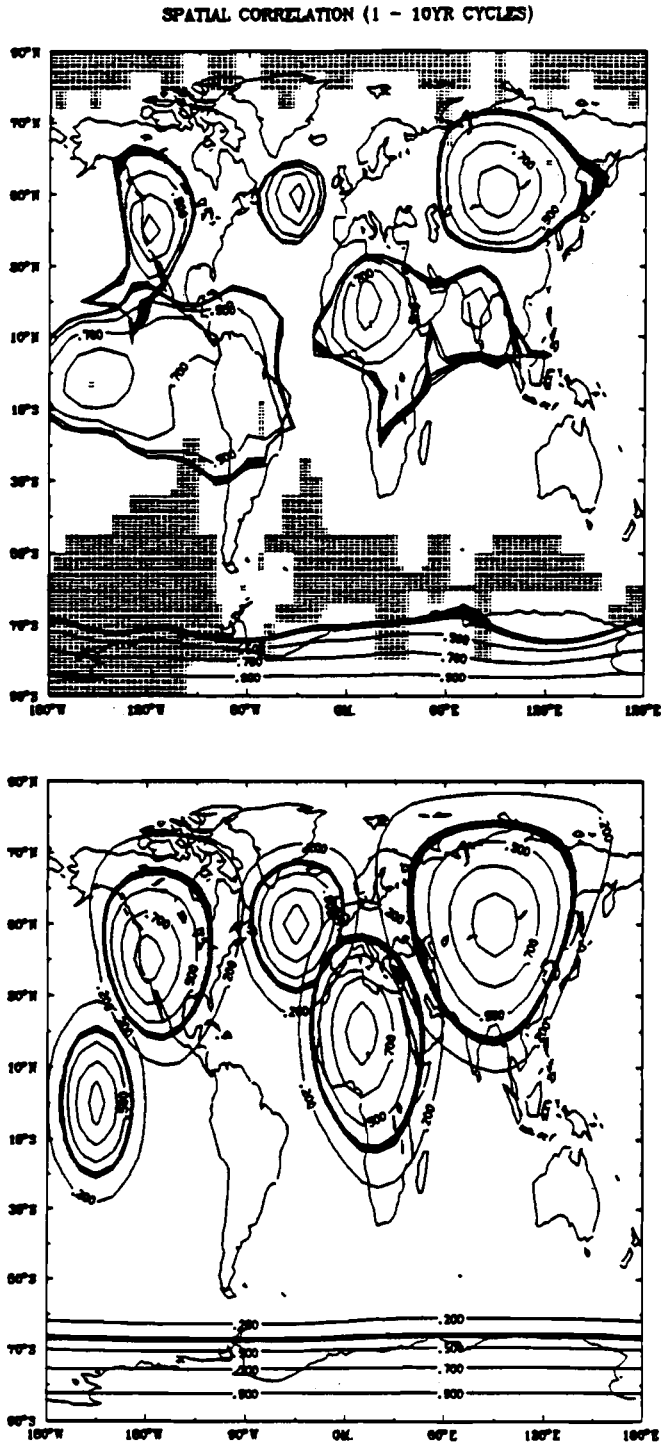

Fig. 6. Spatial correlations of fluctuations within 1 year – 10 year band (annual average temperature field) at selected sampling points: a) observations (shaded areas indicate regions with less than 30 years of data available); b) linear energy balance model with a noise forcing white in space and time.

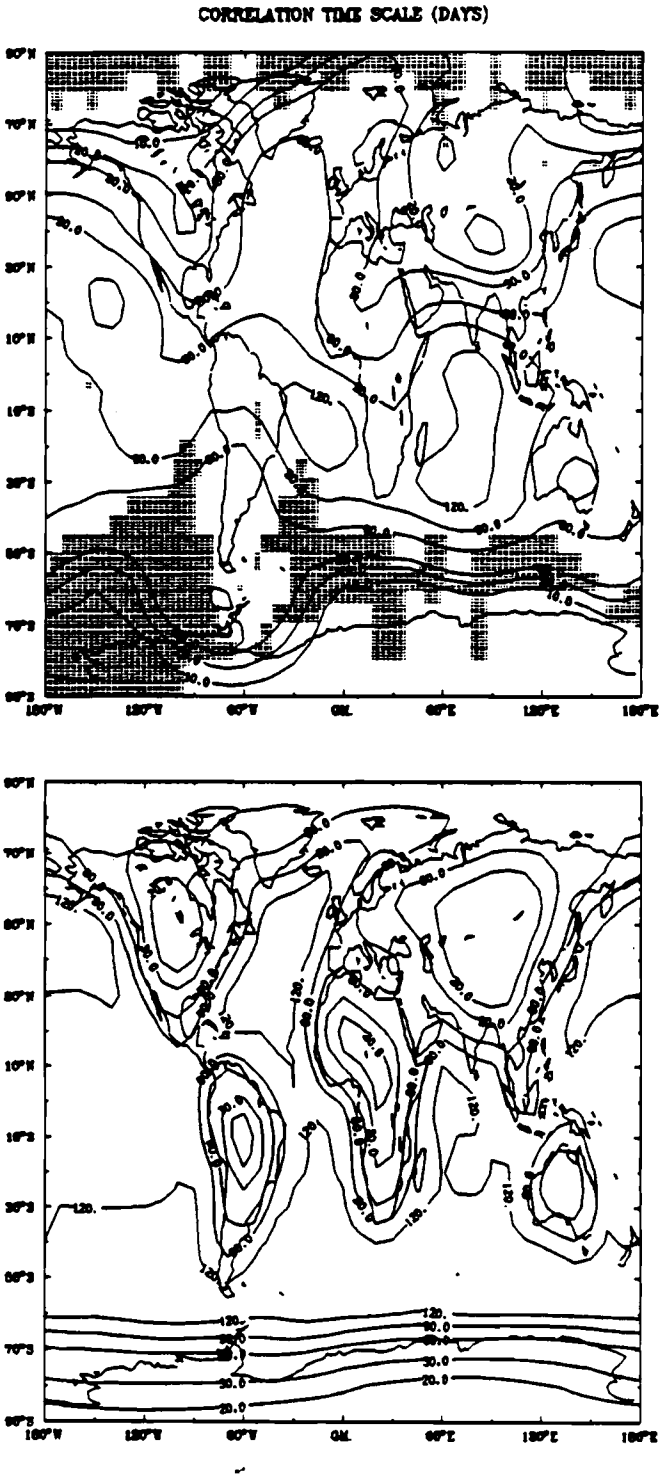

Fig. 7. Correlation time scale (defined as the $1/e$ point of decay) of the response within 2 month - 10 year band: a) observation (moving averaged over a 50° × 25° box; shaded areas indicate regions with less than 30 years of data available); b) linear energy balance model with a noise forcing white in space and time.

APPENDIX B

CLIMATE MODELING DEFINITIONS

APPENDIX B

CLIMATE MODELING DEFINITIONS

B.1 INTRODUCTION

A GLOBAL CLIMATE MODEL is a mathematical computer model that is capable of simulating the seasonal cycle of certain weather variables starting with the planetary scales of atmospheric behavior and including other scales down to some "resolution". These models must be run long enough on the computer for transient effects to die out. An annual cycle model typically uses a simple 50 - 75 meter deep ocean for the lower boundary constraint on the atmosphere. Simulations with these models take a minimum of 15 model years. An imitation of a part of the seasonal cycle can be had by setting the sun at its January position, for example, and prescribing the sea surface temperature for that month from data. While the verisimilitude of this imitation is a matter of dispute it cuts down computer time by about a factor of 20 and it may be valuable for certain purposes. Global atmospheric models have to use other boundary conditions as input, such as the placement and thickness of ice sheets, the atmospheric composition and the oceanic structure. The output of a global climate model is the seasonal cycle in each grid box over the earth. We call this the regional climate forecast.

Examples of global models used in this study:

EBM. EBM is a generic term for an "energy balance model", which calculates temperature as a function of the incoming solar radiation, modified by the albedo (reflectivity) of the earth. In our report, we focus strictly on seasonal models, which involve realistic seasonal forcing and response (as opposed to annual-averaged forcing).

We also use only two-dimensional models, with the dimensions being equivalent to latitude and longitude so that continental outlines can be resolved (this step is necessary because it can be demonstrated that land-sea distribution represents the principal control of seasonal temperature fluctuations). There are several different types of EBMs that we discuss and employ:

LINMOD. LINMOD is the basic version of the 2D-EBM from which others are derived. It was developed by North et al. (1983) and resolves the seasonal cycle but is a linear model and does not allow for the regionally varying albedo of snow and ice.

LINEBM. LINEBM is a modification of LINMOD that allows for regionally varying but prescribed albedo of snow and ice. This model, which is linear, was developed at ARC, described in Hyde et al. (1989), and tested against general circulation model (GCM) simulations of climate change over the last 18,000 years.

NEQMOD. NEQMOD is a model recently completed under this PNL contract. The abbreviation stands for Nonlinear EQuilibrium MODel, for it is a nonlinear model that allows for interactions of altered seasonally varying snow and ice fields with the planetary radiation budget. Such a model is important for testing, for example, the future effect of greenhouse gas changes on climate, for much of the climate system response is nonlinear and involves the snow and ice fields. The "equilibrium" term in the title refers to the fact that there are two different methods of solution for the ice-albedo feedback, one involving spherical harmonic expansions in order to achieve an equilibrium solution, the other involving finite-differencing, which determines a time-marching solution.

GCM. GCM stands for General Circulation Model. This class of models solves the standard equations governing

momentum, moisture, etc. and explicitly computes fields such as circulation, precipitation, etc. It therefore provides much more information than an EBM, but at a much-greater cost and presumably is more realistic. At present our project envisions using two different types of GCMs:

LOW-RESOLUTION GCM (LRM). LRM is, as the name implies, a low-resolution version of a GCM. The model has approximately 15° x 15° resolution in the horizontal, with five levels in the vertical, and a simplified radiation code (Otto-Bliesner et al. 1982). All of these features enable the model to be run approximately ten times faster than the high-resolution version. The LRM is an ideal model for testing a range of parameter space values before settling on a few experiments to run with the most comprehensive type of GCM (see below).

HIGH-RESOLUTION GCM. The High-Resolution GCM is, again as the name implies, a high-resolution model, with about a 5° x 5° horizontal resolution and about ten levels in the vertical, and a more complicated radiative code. This model gives the most detailed information about climate change, but is also the most expensive to operate. The model we plan to use later in the project is a version of the Community Climate Model (CCM) from the National Center for Atmospheric Research (NCAR; cf. Ramanathan et al. 1983, Williamson et al. 1987).

MESOSCALE MODEL. Results from global-scale models will be used as input to a finer-mesh regional model being developed at NCAR (Dickinson et al. 1989, Giorgi and Bates 1989, Giorgi 1990). This model is capable of simulating changes on a spatial scale an order of magnitude finer than the GCM and will be used to make the best estimates of precipitation variations at Yucca Mtn.

B.2 REFERENCES

Dickinson, R. E., R. M. Errico, F. Giorgi, and G. T. Bates. 1989. "A regional climate model for the western United States." Climatic Change 15:383-422.

Giorgi, F. 1990. "Simulation of regional climate using a limited area model nested in a general circulation model." J. Clim. (in press).

Giorgi, F., and G. T. Bates. 1989. "The climatological skill of a regional model over complex terrain." Mon. Wea. Rev. 117:2325-2347.

Hyde, W. T., K.-Y. Kim, G. R. North, and T. J. Crowley. 1989. "Comparison of GCM and energy balance model simulations of seasonal temperature changes over the past 18,000 years." J. Clim. 2:864-887.

North, G. R., J. G. Mengel, and D. A. Short. 1983. "Simple energy balance model resolving the seasons and the continents: Application to the astronomical theory of the ice ages." J. Geophys. Res. 88:6576-6586.

Otto-Bliesner, B. L., G. W. Branstator, and D. D. Houghton. 1982. "A global low-order spectral general circulation model. Part I: Formulation and seasonal climatology." J. Atmos. Sci. 39:929-948.

Ramanathan, V., E. J. Pitcher, R. C. Malone, and M. L. Blackmon. 1983. "The response of a spectral general circulation model to refinements in radiative processes." J. Atmos. Sci. 40:605-630.

Williamson,D. L., J. T. Kiehl, V. Ramanathan, R. E. Dickinson, J. J. Hack. 1987. Description of NCAR Community Climate Model (CCM1). NCAR/TN-285+STR, NCAR Technical Note, 112 pp. National Center for Atmospheric Research, Boulder, Colorado.

PNL-9415
UC-603

Distribution

No. of Copies	OFFSITE
2	DOE Office of Scientific and Technical Information

No. of Copies	ONSITE	
10	Pacific Northwest Laboratory	
	W. H. Walters (7)	K6-60
	Publishing Coordination Technical Report Files (3)	